Received: 22 May 2021 | Revised: 10 January 2022 | Accepted: 16 January 2022

DOI: 10.1002/mp.15494

TECHNICAL NOTE

MEDICAL PHYSICS

Technical note: Controlling the attenuation of 3D-printed physical phantoms for computed tomography with a single material

Huayu Tong[1] | **Hope Pegues**[2] | **Ehsan Samei**[1] | **Joseph Y. Lo**[2] | **Benjamin J. Wiley**[1]

[1]Department of Chemistry, Duke University, Durham, North Carolina, USA

[2]Medical Physics Graduate Program, Department of Radiology, Carl E. Ravin Advanced Imaging Laboratories, Duke University School of Medicine, Durham, North Carolina, USA

Correspondence
Benjamin J. Wiley, Department of Chemistry, Duke University, 124 Science Drive, Box 90354, Durham, NC 27708, USA.
Email: benjamin.wiley@duke.edu

Funding information
NIH/NIBIB, Grant/Award Number: R21EB025549

Abstract

Purpose: The purpose of this work was to characterize and improve the ability of fused filament fabrication to create anthropomorphic physical phantoms for CT research. Specifically, we sought to develop the ability to create multiple levels of X-ray attenuation with a single material.

Methods: CT images of 3D printed cylinders with different infill angles and printing patterns were assessed by comparing their 2D noise power spectra to determine the conditions that produced minimal and uniform noise. A backfilling approach in which additional polymer was extruded into an existing 3D printed background layer was developed to create multiple levels of image contrast.

Results: A print with nine infill angles and a rectilinear infill pattern was found to have the best uniformity, but the printed objects were not as uniform as a commercial phantom. An HU dynamic range of 600 was achieved by changing the infill percentage from 40% to 100%. The backfilling technique enabled control of up to eight levels of contrast within one object across a range of 200 HU, similar to the range of soft tissue. A contrast detail phantom with six levels of contrast and an anthropomorphic liver phantom with four levels of contrast were printed with a single material.

Conclusion: This work improves the uniformity and levels of contrast that can be achieved with fused filament fabrication, thereby enabling researchers to easily create more detailed physical phantoms, including realistic, anthropomorphic textures.

KEYWORDS
3D printing, computed tomography, physical phantom

1 | INTRODUCTION

Computed tomography (CT) is used to diagnose and screen for a variety of conditions of the head, chest, abdomen, pelvis, and spine.[1] Given the important role played by CT imaging and the potential radiation risk, it is critical that the lowest possible dose be used to meet clinical needs. Since humans cannot be used to optimize CT imaging protocols due to radiation concerns and lack of objective ground truth, phantoms are used to test image quality.[2] Commonly used imaging phantoms lack the physical realism necessary to evaluate the ability of a new imaging system or algorithm to detect clinically relevant tasks such as a small, low-contrast lesion in the complex three-dimensional matrix that is the human body, let alone account for variability in body structure across a patient population.

Virtual phantoms have been developed to create more anatomically realistic images for testing CT imaging systems.[3,4] Although virtual phantoms are more realistic than commonly used physical phantoms, virtual phantom simulations necessarily involve approximations and corrections to account for imaging processes that are difficult to model or are proprietary. Therefore,

it may be necessary to use anthropomorphic physical phantoms that are scanned on clinical systems.

Over the last decade, researchers have made great advances in leveraging additive manufacturing to convert virtual phantoms into physical phantoms with increasing accuracy and realism.[5] Methods to convert virtual phantoms to physical phantoms for X-ray imaging include inkjet printing of photocurable resins,[6] inkjet printing on paper,[7] and fused filament fabrication.[8–10] Each method has advantages and disadvantages. Inkjet printing of resins can provide a phantom with features down to ~200 μm, but current commercially available printers (e.g., Polyjet) cost tens to hundreds of thousands of dollars and are closed systems in that they do not allow the owner to use custom inks or printing processes. Inkjet printing on paper is a much cheaper method that also has high resolution, but there are no commercially available systems to automate the stacking and alignment of many pieces of paper to create a phantom. It can also be challenging to load inkjet inks with sufficient material to provide contrast without negatively affecting the printability of the ink. As paper is used as a substrate, it may be challenging to create a phantom with a low attenuation, such as for the lungs.

Fused filament fabrication (FFF), also known as fused deposition modeling (FDM), can create relatively large objects in a fully automated manner.[11] Although the printing resolution may be limited to 0.5 mm for hobby-level 3D printers, higher resolutions (50–100 μm) can be achieved by higher quality machines. The polymers used for FFF are very low in cost, and the open nature of FFF systems makes it easy to create new materials to mimic the X-ray contrast of different parts of the human body.

To date, studies of FFF for X-ray phantoms have determined the attenuation values for different 3D printing materials and infill densities and printed 3D models to mimic the shape of bones, arteries, a skull, and the lungs.[8–10,12,13] One issue with the FFF models created to date is that they contain two or fewer contrast levels in the same print by either using different materials[9] or different infill densities.[8] If the default printer settings are used for such prints, the printer will create a solid shell at the boundary between the materials, which negatively impacts the realism of the model.[10] In addition, the infill printing pattern is clearly visible in most 3D models reported to date, which results in a distracting texture that does not mimic a uniform background.

This paper examines what combination of infill angle and infill pattern most closely mimics a uniform background that minimizes FFF printing artifacts. In addition, we introduce a new approach called backfilling that enables printing multiple contrast levels in one object using a single material while achieving a smoother transition between the contrast levels. These methods are combined to 3D print a contrast detail phantom and liver phantom with multiple levels of contrast, both with a single, standard material. These methods will enable researchers to achieve a new level of anthropomorphic realism with low-cost FFF printers without the need to create custom 3D printing materials.

2 | MATERIALS AND METHODS

2.1 | CT imaging

CT images were acquired with a Discovery 750 HD from GE Healthcare using the standard chest protocol with tube potential of 120 kV and current of 100 mA. An axial scan mode was used. The rotation time was 0.4 s. The CT slice thickness was 0.625 mm. The filtered backprojection algorithm with STANDARD reconstruction kernel was used for every image. As an example of a commercial phantom made of uniform, tissue-equivalent material, a CT phantom insert representing blood (Multi-Energy CT Phantom, Gammex Inc., Middleton WI) was imaged with the printed objects as a control. The CT images shown are all single CT slices. The HU values are averaged over 20 slices. The standard deviation is averaged over 20 standard deviation numbers in each CT slice.

2.2 | NPS analysis

The uniformity of the CT images was determined by plotting their 2D noise power spectrum (NPS).[14] The NPS analysis of the print was performed on 20 CT slices for each object using imQuest available via TG233.[15]

2.3 | 3D printing

The FFF printing process involves creating a 3D model, converting it to an STL file, and converting the STL file to G-CODE instructions for the 3D printer. All the models, with the exception of the liver, were designed in Fusion 360 (Autodesk, San Rafael CA) and exported as an STL file for slicing. The STL files were sliced by Simplify3D (Simplify3D Software, Cincinnati OH) and exported as G-CODE for printing with a PRUSA MK3 (Prusa Research a.s. Czech Republic). The filament used throughout the study was polylactic acid (PLA, MatterHackers Inc. Lake Forest, CA, pro series silver) with a diameter of 1.75 mm.

For FFF printing, the filament is extruded through a heated nozzle (the print head) and deposited on a substrate as lines. The infill angles control the direction of the extruded lines, and the infill pattern controls the pattern of the lines in one layer. The infill percentage is the amount of material that occupies the internal part of the print. By varying the infill percentage, one can change the amount of material deposited at the desired region.

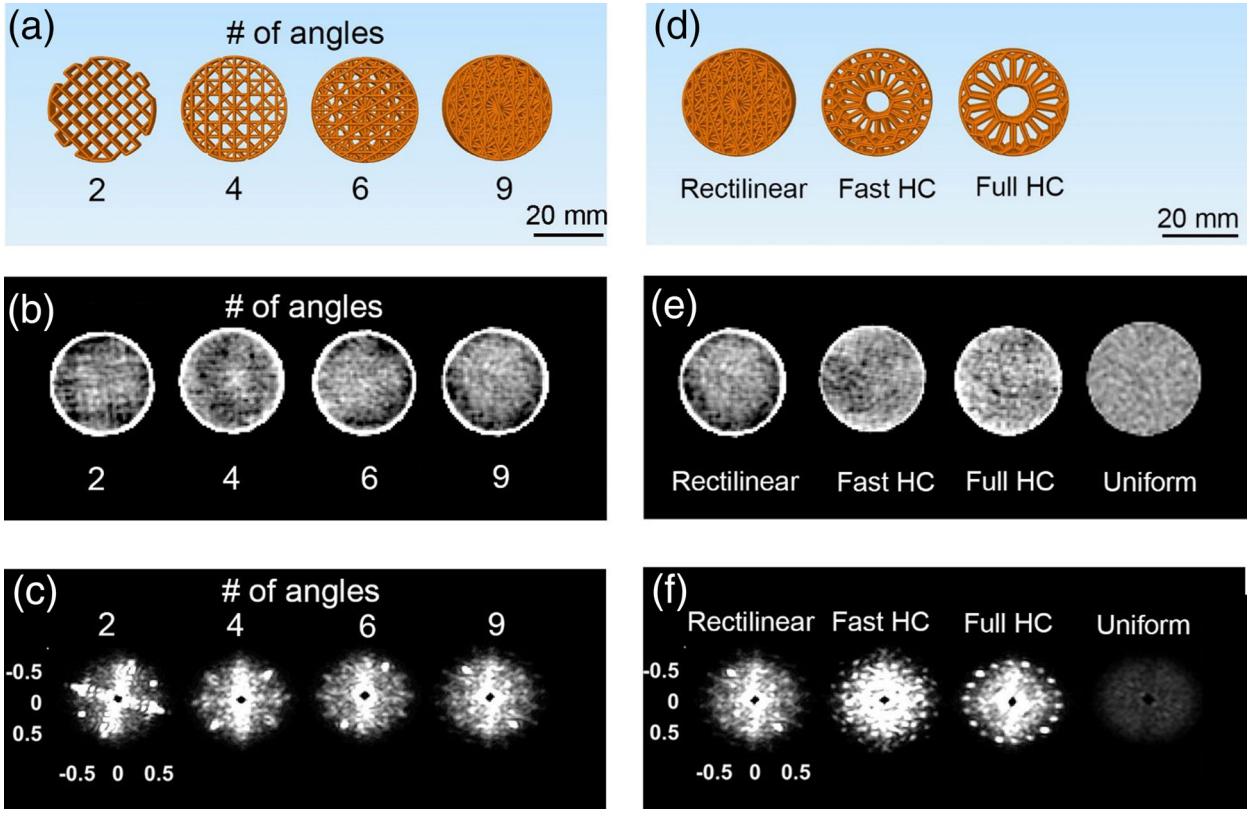

FIGURE 1 (a) Simplify3D software images for a rectilinear pattern with 2, 4, 6, or 9 infill angles and a 10% infill percentage for a cylinder 30 mm in diameter and 20 mm in height. (b) Single-slice (0.625 mm-thick) CT images of cylinders printed with the different infill angles shown in A but with 80% infill. The CT image window width is 50 HU. (c) 2D NPS of the cylinders in Figure 1b. (d) Simplify3D software images for different infill patterns. (e) CT image with a window width of 50 HU. (f) 2D NPS of cylinders with rectilinear, Fast Honeycomb, or Full Honeycomb infill patterns, printed with nine angles and 80% infill. A "uniform" commercial phantom representing blood is included in E&F for comparison. The NPS window is [0,100] for all objects, and the units are mm^{-1}

The infill percentage can be varied from 0% (hollow) to 100% (solid).

All prints were performed with a layer thickness of 0.2 mm, a printing temperature of 200°C, a bed temperature of 60°C, and a nozzle diameter of 0.4 mm. These are default print settings. All models were printed without a solid top and with three bottom layers with 100% infill. The printing speed was 20 mm per min for the first layer and 60 mm per min for the subsequent layers. The fan speed was 0 for the first layer and 100% for the other layers. A cylinder 30 mm in diameter and 0.4 mm in height was printed in parallel with the object to enable the nozzle temperature to reach steady state after the fan was turned on between the first and second layers, i.e., the second layer of the 30 mm cylinder was printed before the second layer of the object.

The shell is a solid outline extruded on the outer surface of the object, serving as the outer wall of the print. The existence of a shell usually results in a high-density wall between two objects or surfaces. For printing the two-level contrast model with shell or no shell, a 3D model of a cylinder 20 mm in diameter and a ring with an outer diameter of 30 mm and an inner diameter of 20 mm was loaded into Simplify3D. The inside cylinder and outside ring were assigned an infill percentage of 80% and 85%, respectively. For printing the model with the shell, the number of shells was 1, and the outline overlap was 15%. For the print with no shell, the outline overlap was 99%.

For the process of backfilling, which is essentially printing twice in the same location, a model for the background and a separate model for the backfilled volume were loaded into the software at the same time. We start with a background layer that has an infill percentage of 80% (HU = –150) and backfill in order to achieve the range of -150 to +50 HU that is typical for a human organ.[16] The infill percentage for the backfilling step was chosen to be 60% to ensure that the print pattern was not visible. However, printing one layer within another will increase the height of the backfilled region, so the extrusion multiplier, which controls the material flow rate, must be reduced from the default value of 1 to prevent the printer nozzle from colliding with the backfilled region. From empirical testing, extrusion multiplier values between 0.1 and 0.4 avoided collision while extruding a consistent, continuous filament during printing.

For the contrast detail phantom, a cylinder 165 mm in diameter was printed as the background with an infill of 80%. Five backfilling processes were printed on the background with an extrusion multiplier between 0.1 and 0.3 with an increment of 0.05.

To create the liver model, one CT slice of an XCAT Phantom was manually segmented into three ranges denoted as "low" (184-224 HU), "high" (225-495 HU), and "all" (-50-495 HU).[3] Each segmented image was converted into STL format and then loaded into Simplify3D for printing. The liver was embedded in a background cylinder with a diameter of 190 mm and an infill of 70% to avoid imaging artifacts. The "all" surface was printed with an extrusion multiplier of 0.15 to provide the cylinder background. The "high" and "low" surfaces were printed with extrusion multipliers of 0.25 and 0.15, respectively, on the "all" section to achieve the desired anthropomorphic pattern.

3 | RESULTS

3.1 | Uniformity

Before modifying the HU values of the phantoms, we first sought to create a phantom with a uniformity approaching that of a commercial phantom. Figure 1a shows images taken from the Simplify 3D software showing how changing the number of infill angles changes the appearance of a rectilinear infill pattern. The lines in this image are the path taken by the 3D printer's extruder. Note that the software image shows a 10% infill to better visualize the print plan, but the actual cylinder was printed with 80% infill. As can be seen in Figure 1a–c, a commonly used rectilinear infill pattern with two-angles is clearly visible in the CT image, and there is a strong cross-like pattern in the 2D NPS. By averaging over up to nine infill angles, the infill pattern was no longer visible in the CT image, and the background appeared more random. The 2D-NPS pattern also showed less structure noise except for a peak at one specific frequency (approximately 0.5 mm^{-1}). Based on these results, nine infill angles were used for the rest of the printed objects discussed in this study.

The print pattern also has an effect on the uniformity of the CT image. Figure 1d–f compares a rectilinear infill pattern to fast honeycomb (Fast HC) and full honeycomb (Full HC). The rectilinear pattern with nine angles is the most uniform based on a visual assessment of the 2D NPS.

3.2 | Creating multiple levels of contrast

A simple way to control the attenuation value of a print is to change the infill density.[8–10,12,13] Figure 2 illustrates the effect of the infill percentage on the appearance and the HU value of test cylinders (20 mm in diameter and 30 mm in height). When the infill percentage is below 40%, the print pattern is easily visible in the CT image, a condition that makes this infill percentage unsuitable for mimicking the texture of tissue. Figure 2d shows that there is a linear relationship between the attenuation and the infill percentage. The typical attenuation range

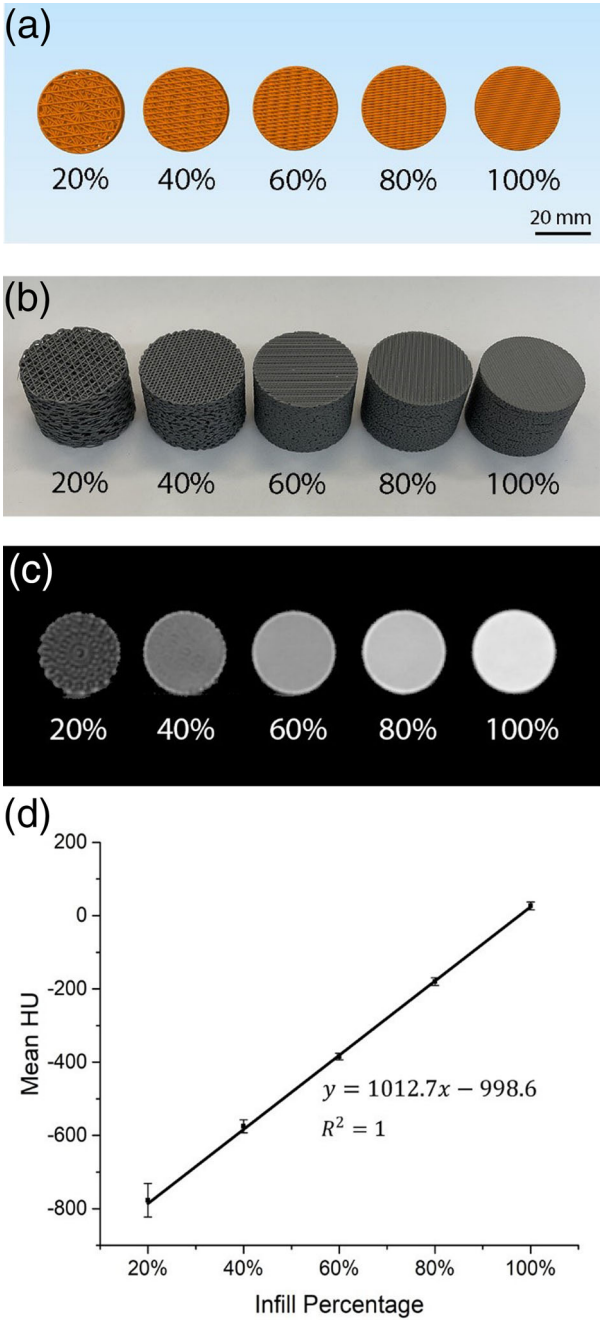

FIGURE 2 (a) Simplify3D software images of cylinders with different infill percentages for test cylinders 30 mm in diameter and 20 mm in height. All cylinders were printed using nine random infill angles. (b) Camera images of cylinders with different infill percentages. (c) CT image of cylinders with infill percentages ranging from 20% to 100%. The window width is 1250 HU. (d) The linear fit between mean HU and the infill percentage.

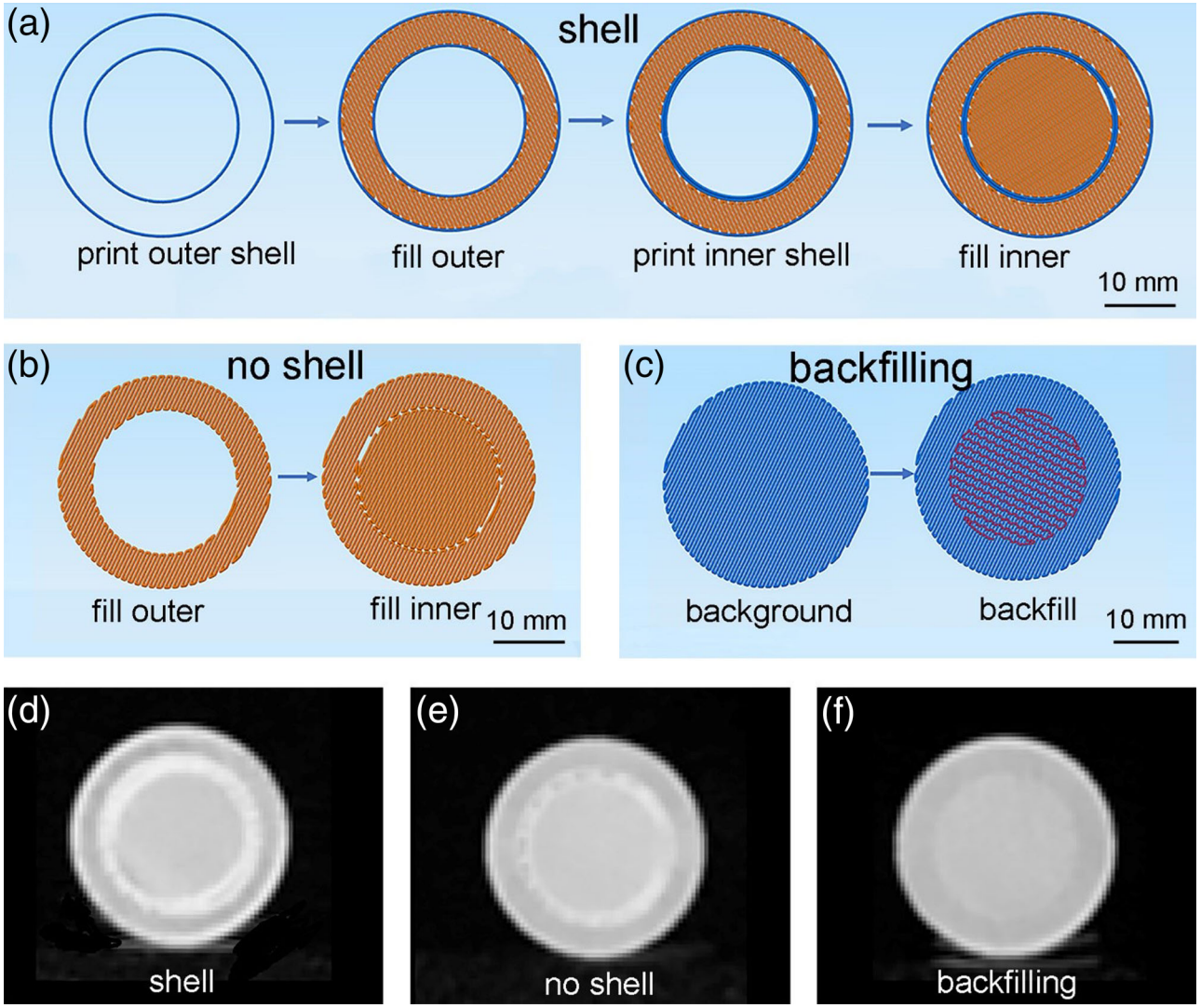

FIGURE 3 Simplify3D software images for prints with (a) shell, (b) no shell, and (c) backfilling. (d–f) The corresponding CT images with a window width of 1250 HU. The outer ring or background regions were printed with nine infill angles and 80% infill with a rectilinear pattern. Shell and no shell are printed with a rectilinear pattern and infill percentages of 85% in the center. The backfilled region was printed with a 60% infill and Fast HC pattern with an extrusion multiplier of 0.2

for soft tissue is –150 to +50 HU. This same range of contrast can be achieved using 80% to 100% infill.

Although the infill percentage can create multiple levels of contrast in the same object, it is challenging to make a smooth transition between different infill percentages. The default approach to printing multiple levels of contrast is shown in Figure 3a for a cylinder with two infill percentages. The software creates a two-layer-thick shell between the two areas of infill, which appears as a bright line in the CT image (Figure 3d). If the shell is removed (Figure 3b), there is still a third level of contrast between the two cylinders (Figure 3e). The presence of a shell in the CT image of the "no shell" cylinder is due to an artifact of the printing process. Figure 3b shows that the path taken by the 3D printer extruder results in U-turns at the interface between the inner and outer shell. Excess material tends to be extruded at these turning points, resulting in the observed shell.

To address this issue, we devised the backfilling method illustrated in Figure 3c, in which we first print a background layer and then extrude additional polymer into a desired region. Backfilling is essentially printing twice in the same position. As shown in Figure 3f, this method allows one to achieve two adjacent regions with different densities without an additional boundary in the transition region.

Figure 4a shows the linear relationship between the extrusion multiplier, a number that controls the material flow rate, used during backfilling and the corresponding HU value of the backfilled region. The standard deviations indicate that regions with an extrusion multiplier difference of 0.05 will have a measurable difference in

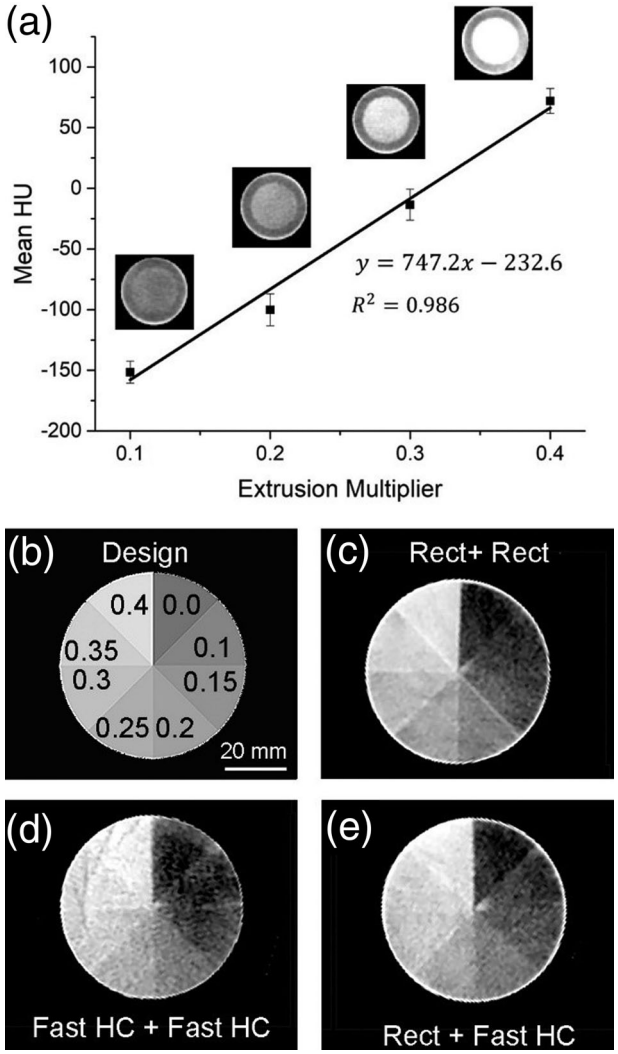

FIGURE 4 (a) Calibration fit for the HU value vs. extrusion multiplier. (b) Design of an 8-piece-pie denoting regions with different extrusion multipliers. (c–e) CT images of printed pies with different infill patterns. The CT window width was 250 HU for all images.

their HU value. This suggests that the backfilling method can create objects with up to eight levels of contrast with a single material. To test this possibility, we created a pie model (Figure 4b) wherein each backfilled slice of the pie used a different extrusion multiplier value. Figure 4c shows the CT image of the model created with a rectilinear printing pattern. Although eight contrast levels are clearly visible in the CT image, there is also a thin line of higher contrast between the printed regions due to the overextrusion from the nozzle when it changed directions. Switching the background and backfill pattern to Fast HC removed the problem of the high contrast boundary. However, the Fast HC method results in dark line artifacts visible in the print (upper left of Figure 4d) due to underextrusion when a new extrusion process starts. Using a rectilinear background with a fast HC infill can reduce both the high-contrast boundary and the dark line artifacts. This printing approach allows up to eight levels of contrast with a smooth transition between adjacent regions.

3.3 | Phantom applications

To demonstrate the clinical utility of this new printing methodology, we fabricated a contrast detail phantom containing targets with sizes and contrast levels embedded in a uniform background. Figure 5 shows the design and resulting CT image of our contrast detail phantom, which contains five different contrast levels and four different sizes of cylindrical objects ranging from 3 to 20 mm.

As a second application, we demonstrate the printing of an anthropomorphic phantom based on a virtual XCAT liver phantom (Figure 6a). The three contrast levels were printed with three backfilling processes on a cylindrical background, as illustrated by the design in Figure 6b. As can be seen in the resulting CT image of the printed liver phantom (Figure 6d), the details of the patient liver were replicated by the printed liver phantom.

4 | DISCUSSION

In an attempt to address the lack of realistic commercial phantoms, this study proposes new methods to fabricate physical phantoms with anthropomorphic structures and multiple levels of contrast. Previous FFF-based phantoms were limited by the relatively simple printing pattern, resulting in obvious linear texture artifacts visible in the resulting CT image.[9,10] We addressed this problem by increasing the infill angles and optimizing the infill pattern during the printing process. Previous studies reported that the contrast level of the print can be changed by using different materials or by changing the infill percentage.[8–10,12,13] A different artifact arises, however, because current FFF phantoms do not have a smooth transition between two contrast levels. Our proposed backfilling method solves this problem. Unlike previous reports limited to two contrast levels,[9,10] our method can print up to eight levels of contrast in a single object.

The usefulness of our proposed techniques was demonstrated by designing and fabricating two medical imaging phantoms. First, we created a contrast-detail phantom. Unlike commercial phantoms that can cost thousands of dollars, this 3D-printed one can be created in 24 h for approximately $20 in material. Second, we showcased the ability of FFF to reproduce anthrophonic structures by creating a liver phantom with four levels of contrast and irregular shape. Such fabricated phantoms can be used in CT research, including task-specific assessment of imaging technology or patient-specific optimization of acquisition protocols.

This study has several limitations. First, even after the optimization of the printing parameters, the 3D printed

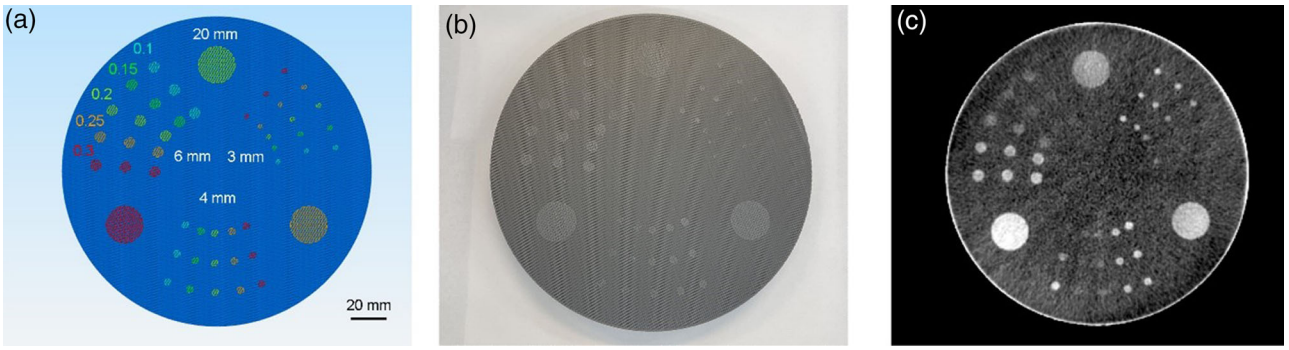

FIGURE 5 (a) Simplify3D software image showing the dimensions of the printed areas. (3–20 mm). The different colors in (a) represent different printing processes with extrusion multipliers of 0.1, 0.15, 0.2, 0.25, and 0.3. (b) Optical image of the contrast detail phantom. (c) CT image with a window width of 280 HU

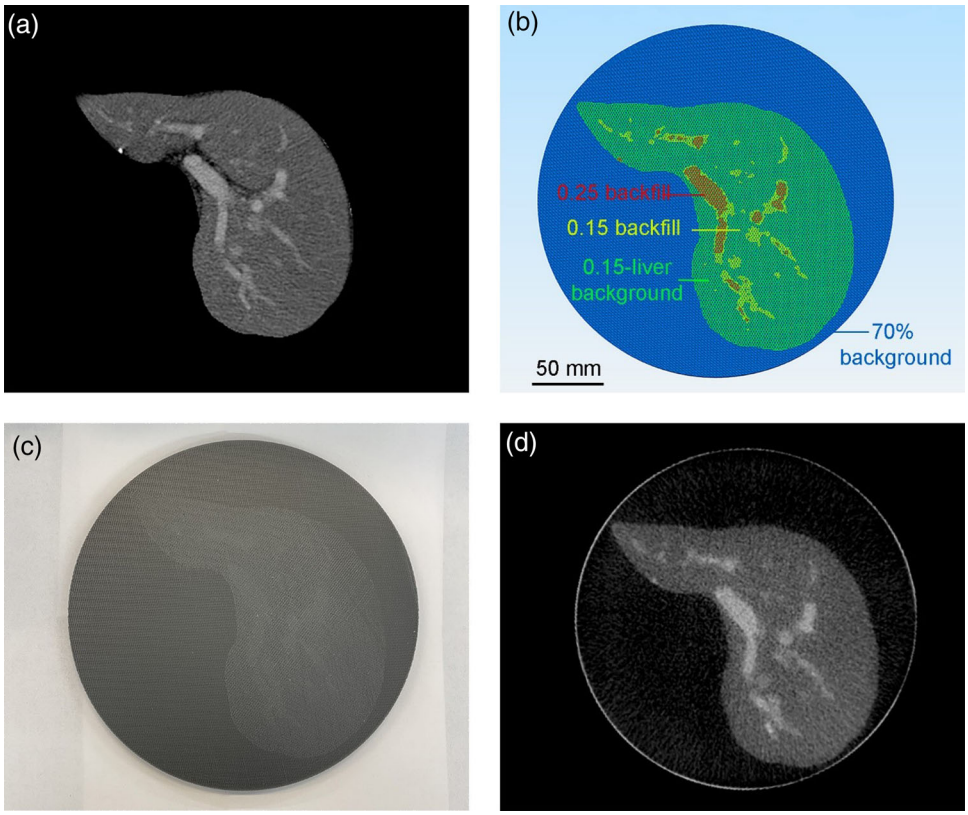

FIGURE 6 (a) Simulated CT image of the virtual XCAT liver phantom. (b) Software design of the liver phantom. (c) Optical image of the printed liver phantom. (d) CT image of the printed liver phantom with a window width of 350 HU. The phantom was printed with a 70% infill, rectilinear pattern for the cylinder, 60% infill, Fast HC pattern with an extrusion multiplier of 0.15 for the liver background, and 60% infill, Fast HC with an extrusion multiplier of 0.15 and 0.25 for the low contrast and high contrast regions, respectively

phantoms are less uniform than the commercial phantom used for comparison. Additional work is necessary to determine the impact of the less uniform 3D-printed phantoms on CT measurements. The resolution of the current printer also makes it difficult to backfill regions less than 2 mm in diameter. A higher resolution FDM printer with a smaller nozzle size and finer motor control may address these problems, with the tradeoff of longer printing time and higher printer cost.

Currently, we are using a single material to provide the attenuation difference within the CT image. However, dual energy or photon counting CT requires discerning other materials, such as iodine or calcium. This can be potentially solved by multimaterial printing using commercial or customized filaments.

5 | CONCLUSION

By demonstrating a new method to obtain up to eight levels of contrast with a single material, this study has improved the ability of fused filament fabrication to create realistic physical phantoms for CT imaging research. This study also describes the printing parameters that optimize the uniformity of a printed phantom area and how to obtain smooth transitions between areas with different HU values. The utility of these methods was demonstrated by creating a contrast detail phantom with six levels of contrast and an anthropomorphic liver phantom with four levels of contrast. The low-cost and easily customizable phantoms described here could facilitate the improvement of CT imaging protocols and the characterization of CT imaging systems.

ACKNOWLEDGEMENTS

The authors thank Justin Solomon and Michael Gehm for helpful discussions and Cindy Davis for facilitating CT scanning sessions. This work was funded in part by NIH/NIBIB R21EB025549.

CONFLICTS OF INTERESTS

Joseph Lo has a license agreement with Gammex Inc./Sun Nuclear regarding intellectual property that may be related to this study. Ehsan Samei lists relationships with the following entities unrelated to the present publication: GE, Siemens, Bracco, Imalogix, 12Sigma, SunNuclear, Metis Health Analytics, Cambridge University Press, and Wiley and Sons.

DATA AVAILABILITY STATEMENT

The data that support the findings of this study are available from the corresponding author upon reasonable request.

REFERENCES

1. Tepper SJ. Computed tomography: an increasing source of radiation exposure – commentary. *Headache*. 2008;48:657.
2. Robinson D. The phantoms of medical and health physics. *Med Phys*. 2016;43:5264-5264.
3. Segars WP, Mahesh M, Beck TJ, Frey EC, Tsui BMW. Realistic CT simulation using the 4D XCAT phantom. *Med Phys*. 2008;35:3800-3808.
4. Abadi E, Segars WP, Tsui BMW, et al. Virtual clinical trials in medical imaging: a review. *J Med Imaging*. 2020;7:1-40.
5. Filippou V, Tsoumpas C. Recent advances on the development of phantoms using 3D printing for imaging with CT, MRI, PET, SPECT, and ultrasound. *Med Phys*. 2018;45:e740-e760.
6. Rossman AH, Catenacci M, Zhao C, et al. Three-dimensionally printed anthropomorphic physical phantom for mammography and digital breast tomosynthesis with custom materials, lesions, and uniform quality control region. *J Med Imaging*. 2019; 6:1.
7. Jahnke P, Schwarz S, Ziegert M, et al. Paper-based 3D printing of anthropomorphic CT phantoms: feasibility of two construction techniques. *Eur Radiol*. 2019;29:1384-1390.
8. Hong D, Lee S, Kim GB, et al. Development of a CT imaging phantom of anthromorphic lung using fused deposition modeling 3D printing. *Medicine (Baltimore)*. 2020;99:e18617.
9. Ceh J, Youd T, Mastrovich Z, et al. Bismuth infusion of ABS enables additive manufacturing of complex radiological phantoms and shielding equipment. *Sensors (Switzerland)*. 2017;17:1-11.
10. Hamedani BA, Melvin A, Vaheesan K, et al. Three-dimensional printing CT-derived objects with controllable radiopacity. *J Appl Clin Med Phys*. 2018;19:317-328.
11. Singh S, Singh G, Prakash C, Ramakrishna S. Current status and future directions of fused FI lament fabrication. *J Manuf Process*. 2020;55:288-306.
12. Dancewicz OL, Sylvander SR, Markwell TS, Crowe SB, Trapp JV. Radiological properties of 3D printed materials in kilovoltage and megavoltage photon beams. *Phys Medica*. 2017;38: 111-118.
13. Ivanov D, Bliznakova K, Buliev I, et al. Suitability of low density materials for 3D printing of physical breast phantoms. *Phys Med Biol*. 2018;63:175020.
14. Williams MB, Mangiafico PA, Simoni PU. Noise power spectra of images from digital mammography detectors. *Med Phys*. 1999;26:1279-1293.
15. Samei E, Bakalyar D, Boedeker KL, et al. Performance evaluation of computed tomography systems: summary of AAPM Task Group 233. *Med Phys*. 2019;46:e735-e756.
16. Toga AW, Mazziotta JC. *Brain Mapping: The Methods*. Elsevier Science; 2002.

How to cite this article: Tong H, Pegues H, Samei E, Lo JY, Wiley BJ. Technical note: Controlling the attenuation of 3D-printed physical phantoms for computed tomography with a single material. *Med Phys*. 2022;49:2582–2589. https://doi.org/10.1002/mp.15494